The emission process of secondary ions from solids bombarded with large gas cluster ions

Satoshi Ninomiya [a]*, Kazuya Ichiki [b], Toshio Seki [b,d], Takaaki Aoki [c,d], Jiro Matsuo [a,d]

[a] *Quantum Science and Engineering Center, Kyoto University, Gokasho, Uji, Kyoto 611-0011, Japan*

[b] *Department of Nuclear Engineering, Kyoto University, Sakyo, Kyoto 606-8501, Japan*

[c] *Electronic Science and Engineering, Kyoto University, Nishikyo, Kyoto, 615-8510, Japan*

[d] *CREST, Japan Science and Technology Agency (JST), Chiyoda, Tokyo, 102-0075, Japan*

* Corresponding author: Satoshi Ninomiya

Quantum Science and Engineering Center, Kyoto University, Uji, Kyoto 611-0011, Japan

Tel: +81-774-38-3977, FAX: +81-774-38-3978

E-mail address: ninomiya@nucleng.kyoto-u.ac.jp

Abstract:

We investigated the effects of size and energy of large incident Ar cluster ions on the secondary ion emission of Si. The secondary ions were measured using a double deflection method and a time-of-flight (TOF) technique. The size of the incident Ar cluster ions was between a few hundreds and several tens of thousands of atoms, and the energy up to 60 keV. Under the incidence of keV energy atomic Ar ions, atomic Si ions were mainly detected, and Si cluster ions were rarely observed. On the other hand, under the incidence of large Ar cluster ions, the dominant secondary ions were Si_n^+ ($2 \leq n \leq 11$). It has become clear that the yield ratio of secondary Si cluster ions was determined by the velocity of the incident cluster ions, and this

strong dependence of the yield ratio on incident velocity should be related to the mechanisms of secondary ion emission under large Ar cluster ion bombardment.

PACS: 79.20.-m; 79.20.Rf

Keywords: Ar cluster, TOF, Si, Secondary ion, Si cluster

1. Introduction

The collision processes of atomic ions in solids have been investigated in detail for a long time and development of a number of analytical techniques using ion beams followed these studies [1]. Lately, cluster ion interactions with solids have become the center of much attention because of many unique phenomena, not found under atomic and small molecular ion impacts. These phenomena are often called “cluster effects” or “nonlinear effects” and the studies of cluster–solid interactions have also developed rapidly. For instance, secondary ion mass spectrometry (SIMS) with cluster ions such as Au_3^+[2], Bi_5^+[3] and C_{60}^+[4] has been frequently studied, and numerous experimental results have shown that both sputtering and secondary ion yields are significantly enhanced by cluster ion impact compared to atomic ions at the same incident velocity [5,6]. It has also been indicated that emission yields are enhanced with increasing size of the primary cluster ion.

However, there are very few reports about the interactions of extremely large cluster ions with solids. In previous studies, we have reported the unique secondary ion emission for some targets using large Ar cluster ions that are much larger than the molecular ions as primary ions [7–9]. This research is progressing well since it started. In this study, secondary ions were measured for Si bombarded with large, size-selected large Ar cluster ions using a time-of-flight

(TOF) technique. We systematically investigated the effect of primary Ar cluster ion size and energy on the emission yields for Si. The emission processes of secondary ions under large cluster ion bombardment will also be discussed.

2. Experimental

A method for the generation of gas cluster ion beams with high current density (a few $\mu As/cm^2$) has been developed at Kyoto University, and the large cluster formation and ionization techniques were described in previous studies [10,11]. The gas cluster ion beam equipment consists of a source chamber, an ionization chamber and an ultra-high vacuum (UHV) analytical chamber. A differential pumping chamber is placed between the ionization chamber and the UHV analytical chamber. The UHV analytical chamber is equipped with a linear TOF mass spectrometer [12]. Neutral Ar clusters are formed by supersonic expansion of high-pressure gas (8×10^5 Pa) through a nozzle and are then introduced into the ionization chamber. Electrons ejected from a hot filament are accelerated toward the neutral Ar clusters and ionize neutral them. The ionized Ar clusters are extracted towards a target with an accelerating voltage up to 60 kV. Magnets installed in the ionization chamber remove small cluster and atomic ions included in the cluster ion beams. In this study, the maximum current density of the Ar cluster beam was 5 $\mu A/cm^2$, and the mean cluster size was about 2000 atoms/cluster. The primary ion beam was incident on a clean silicon (1 0 0) target at an angle of 45° with respect to the surface normal. The base and working pressures in the UHV analytical chamber were 1×10^{-8} and 2×10^{-7} Pa, respectively.

A double deflection method was employed to measure the size dependence of secondary ion yields under the incidence of large Ar cluster ions [7]. First, the primary ion beam is chopped to

a width of 5 μs every 1 ms by applying a high-voltage pulse (~1000 V) between parallel electrodes (10 mm effective deflector length). When the pulsed ion beam is incident on a target, the beam width spreads beyond 100 μs because of the size difference of the incident cluster ions. Then, secondary ions produced are extracted with an electronic field and reach a second deflector installed between the target and a secondary-ion detector. The second deflector consists of two electrically insulated sets of thin (0.35 mm diameter) parallel wires mounted at a distance of 0.85 mm from each other and perpendicular to the target surface normal on a piece of double-sided circuit board. Finally, secondary ions were chopped to a width of 200 ns every 1 ms by applying a high-voltage pulse (below 500 V) between the wires. We can selectively measure secondary ions produced by cluster ions of different size by changing the time interval (delay time) between the first and second chopping. Secondary ions were extracted with kinetic energy of 2 keV and detected with a microchannel plate (MCP) set on the axis of the surface normal. The timing of the second chopping and secondary-ion detection was respectively used as a start and a stop signal for the TOF mass spectrometry (TOF-MS), and each TOF measurement was taken for 20 s.

3. Results and discussion

Figure 1(a) shows a TOF spectrum of positively charged secondary ions for Si bombarded with 60 keV Ar cluster ions using a simple single deflection TOF method. Because, as mentioned, the first chopping and the secondary-ion detection were respectively, used as a start and a stop signal for the TOF measurement, it was impossible to mass-analyze different secondary-ion species. Therefore, the primary ion beams or secondary-ion species had to be chopped into short pulses again after being chopped with the first primary ion deflector. Fig.

1(b,c) shows the secondary ion spectra using the double deflection method. The delay times from the first chopping were respectively 155 and 500 μs, and this corresponds to Ar_{2000} and Ar_{20000} ions. The main ions detected under the incidence of 60 keV Ar_{2000} ions were atomic Si and cluster ions (Si_n^+, $2 \leq n \leq 11$). Ar^+ and $ArSi^+$ ions were also detected in a small quantity. On the other hand, under the incidence of 60 keV Ar_{20000} ions, the dominant ions detected were $(H_2O)_kH^+$ (k=1–6) and $(H_2O)_lAr_m^+$ (l=1–2, m=1–6) species, and their yields were quite low compared to the incidence of 60 keV Ar_{2000} ions. These ions were not observed for a Si target under the incidence of atomic Ar ions [8,9]. When neutral Ar clusters are formed by supersonic expansion, H_2O molecules included in the source chamber will likely be incorporated into the resultant Ar clusters. Therefore, it seems to be quite logical to consider $(H_2O)_kH^+$ and $(H_2O)_lAr_m^+$ species as projectile-related ions. It is noteworthy that Si-related ions were rarely produced under incidence of Ar cluster ions that were larger than Ar_{5000}.

Figure 2 shows mass spectra of positively charged secondary ions for Si bombarded with (a) 15 keV Ar^+, (b) 40 keV Ar_{500} and (c) 40 keV Ar_{2000} ions. Secondary ions were measured under high vacuum (a, 1×10^{-3} Pa) and UHV conditions (b and c). Under the incidence of 15 keV Ar atomic ions, atomic Si ions were mainly detected, and Si cluster ions were rarely observed. On the other hand, under bombardment with 40 keV Ar_{500} and Ar_{2000} ions, the dominant secondary ions were Si_n^+ up to n=11. However, the emission yields were different with incidence of Ar_{500} and Ar_{2000} clusters. Under Ar_{500} incidence, 50% of the total number of secondary ions were emitted as Si cluster ions and with Ar_{2000} this amount increased to 60%. If the number of Si cluster ions is converted into Si atoms, 79% of the total atom number of secondary ions were emitted as Si cluster ions with Ar_{500} ions, and the ratio reached 87% with Ar_{2000} incidence. Furthermore, the ratio of large Si cluster ions depended on the primary Ar cluster ion species, and 13% of the total atom number of secondary ions were emitted as Si cluster ions larger than

Si_6^+ with Ar_{500} incidence. With Ar_{2000} this ratio was 29%, i.e. more than twice that of Ar_{500}. On the other hand, it has been reported that Si cluster ions are also produced from Si under atomic ion bombardment in the keV range. However, the cluster ion yields are quite low: for instance, under keV energy Ar^+ impact, the cluster ion yield ratio was below 20% [13]. It is considerably important to mention here that under the impact of large Ar cluster ions, most of the secondary ions are emitted as Si clusters.

Next let us evaluate the Si cluster emission yields systematically. The conditions of cluster emission require taking into account the same parameters, incident cluster size and energy. When the yields of secondary ions are discussed, evaluating their production probabilities becomes a serious problem. Particularly, the ionization potential seems to be different between Si atoms and Si clusters. In order to minimize these effects on emission yields, the yields of Si_6^+ relative to those of Si_2^+ were plotted as a function of incident Ar cluster size. Figure 3(a) shows the effect of incident cluster size and energy on the emission yield ratios. Under the same incident ion energy conditions, the yield ratios increased with incident size and gave the maximum value at a certain size, and these maxima depended on incident energy. Under the incidence of 20 keV Ar cluster ions, the yield ratios increased and saturated rapidly with incident size compared to 60 keV. It was found that the yield ratios of secondary cluster ions were not determined by incident cluster size and energy. Figure 3 (b) shows the yield ratios as a function of incident energy per atom of Ar. (The same incident energy per atom condition corresponds to the same incident velocity condition). As is evident from Fig. 3 (b), the yield ratios are surprisingly well expressed as a universal solid line. That is, it becomes clear that the velocity of incident cluster ions determines the yield ratios of secondary cluster ions, and this strong dependence should be related to the mechanisms of cluster emission under large Ar cluster ion bombardment.

Finally, we discuss the mechanisms of cluster emission from solids under the impact of large clusters. When a large cluster is incident on a solid surface, a crater is formed on the surface. The crater formation was confirmed with scanning tunneling microscopy (STM) on highly oriented pyrolitic graphite (HOPG) surfaces irradiated by Ar cluster and C_{60} ions [14,15]. On the other hand, the emission processes of cluster–solid collisions have been recently investigated by computer simulations. Aoki et al. performed molecular dynamics (MD) simulations to study the emission process between a large cluster and a solid surface. MD simulation data provide fundamental understanding on the emission processes of sputtered particles. According to the MD simulations, surface atoms near the edge of the crater are pushed outward soon after the cluster impact [16,17]. Moreover, preliminarily results indicate that the velocity of the edge during cluster impact correlates strongly with the velocity of the incident cluster [18]. That is, the dependence of cluster emission yield ratios on incident velocity obtained by experimental results agrees well with the MD calculation results. Further analysis of these experimental and MD results may reveal that edge velocity plays a major role in secondary particle emission under the impact of large clusters.

4. Summary

Positively charged secondary ions produced from Si were measured using a double deflection method and a TOF technique under the incidence of large Ar cluster ions that consisted of more than 500 atoms. Under the incidence of 15 keV Ar^+ ions, atomic Si ions were mainly detected, and Si cluster ions were rarely observed. On the other hand, under the incidence of 40 keV Ar_{2000} ions, the dominant secondary ions were Si_n^+ up to n=11. From the total atom number of secondary ions, 87% was emitted as Si cluster ions for 40 keV Ar_{2000} incidence. It was found

that the yield ratios of secondary cluster ions were not determined by incident cluster size and energy, but were strongly dependent on the incident energy per atom (velocity) of the large cluster ions. The results presented in this study clearly show that the mechanism of cluster emission is influenced by the velocity of primary Ar cluster ions.

Acknowledgements

This work was supported in part by the Research Fellowships of the Japan Society for the Promotion of Science (JSPS) for Young Scientists. This paper was edited for publication by Edit Associates (http://www.editassociates.com), and the authors gratefully acknowledge its editor-in-chief, Dr. Rafael Manory.

References

[1] M.B.H. Breese, D.N. Jamieson, P.J.C. King, Material Analysis Using a Nuclear Microprobe, Wiley-Interscience, John Wiley & Sons, 1996.

[2] D. Touboul, F. Halgand, A. Brunelle, R. Kersting, E. Tallarek, B. Hagenhoff and O. Laprévote, Anal. Chem. **76** (2004) 1550.

[3] D. Touboul, F. Kollmer, E. Niehuis, A. Brunelle and O. Laprévote, J. Am. Soc. Mass Spectrom. **16** (2005) 1608.

[4] D. Weibel, S. Wong, N. Lockyer, P. Blenkinsopp, R. Hill and J.C. Vickerman, Anal. Chem. **75** (2003) 1754.

[5] R.D. Rickman, S.V. Verkhoturov, E.S. Parilis and E.A. Schweikert, Phys. Rev. Lett. **92** (2004) 047601.

[6] S. Bouneau, A. Brunelle, S. Della-Negra, J. Depauw, D. Jacquet, Y. Le Beyec, M. Pautrat, M. Fallavier, J.C. Poizat and H.H. Andersen, Phys. Rev. B **65** (2002) 144106.

[7] S. Ninomiya, Y. Nakata, K. Ichiki, T. Seki, T. Aoki and J. Matsuo, Nucl. Instr. and Meth. B **256** (2007) 493.

[8] S. Ninomiya, K. Ichiki, Y. Nakata, T. Seki, T. Aoki and J. Matsuo, Nucl. Instr. and Meth. B **256** (2007) 528.

[9] S. Ninomiya, T. Aoki, T. Seki and J. Matsuo, Appl. Sur. Sci. **252** (2006) 6550.

[10] I. Yamada, J. Matsuo, N. Toyoda and A. Kirkpatrick, Mater. Sci. Eng. R **34** (2001) 231.

[11] T. Seki, J. Matsuo, G.H. Takaoka and I. Yamada, Nucl. Instr. and Meth. B **206** (2003) 902.

[12] S. Ninomiya, K Ichiki, Y. Nakata, Y. Honda, T. Seki, T. Aoki and J. Matsuo, Appl. Sur. Sci. **255** (2008) 880.

[13] D. Lipinsky, R. Jede, O. Ganschow and A. Benninghoven, J. Vac. Sci. Technol. A **3** (1985) 2007.

[14] T. Seki, T. Kaneko, D. Takeuchi, T. Aoki, J. Matsuo, Z. Insepov and I. Yamada, Nucl. Instr. and Meth. B **121** (1997) 498.

[15] T. Seki, T. Aoki, M. Tanomura, J. Matsuo and I. Yamada, Mat. Chem. Phys. **54** (1998) 143.

[16] T. Aoki, T. Seki, S. Ninomiya and J. Matsuo, Surf. & Coat. Technol. **201** (2007) 8427.

[17] T. Aoki and J. Matsuo, Nucl. Instr. and Meth. B **216** (2004) 185.

[18] T. Aoki, T. Seki, S. Ninomiya, K. Ichiki, J. Matsuo, Instr. and Meth. B **267** (2009) 1424.

Figure captions

Fig. 1. TOF spectra of positively charged secondary ions for Si bombarded with 60 keV Ar cluster ions using (a) a single deflection method and (b,c) a double deflection method. The incident ions were (b) Ar_{2000} and (c) Ar_{20000} at 60 keV.

Fig. 2. Mass spectra of positively charged secondary ions for Si bombarded with (a) 15 keV Ar^+, (b) 40 keV Ar_{500} and (c) 40 keV Ar_{2000} ions.

Fig. 3. The effects of incident (a) cluster size and energy and (b) energy per atom (velocity) on Si cluster ion yield ratios (Si_6^+/Si_2^+) under the incidence of large Ar cluster ions. The solid line in (b) is drawn to guide the eye.

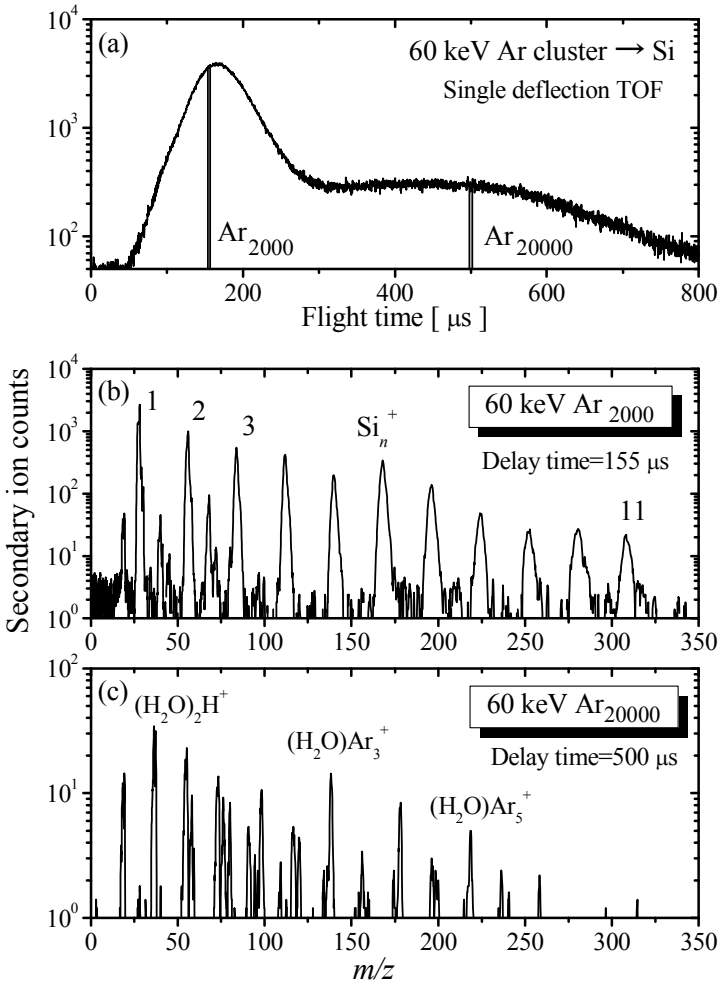

Fig. 1. Ninomiya et al. The emission process of secondary ions from solids bombarded with large gas cluster ions

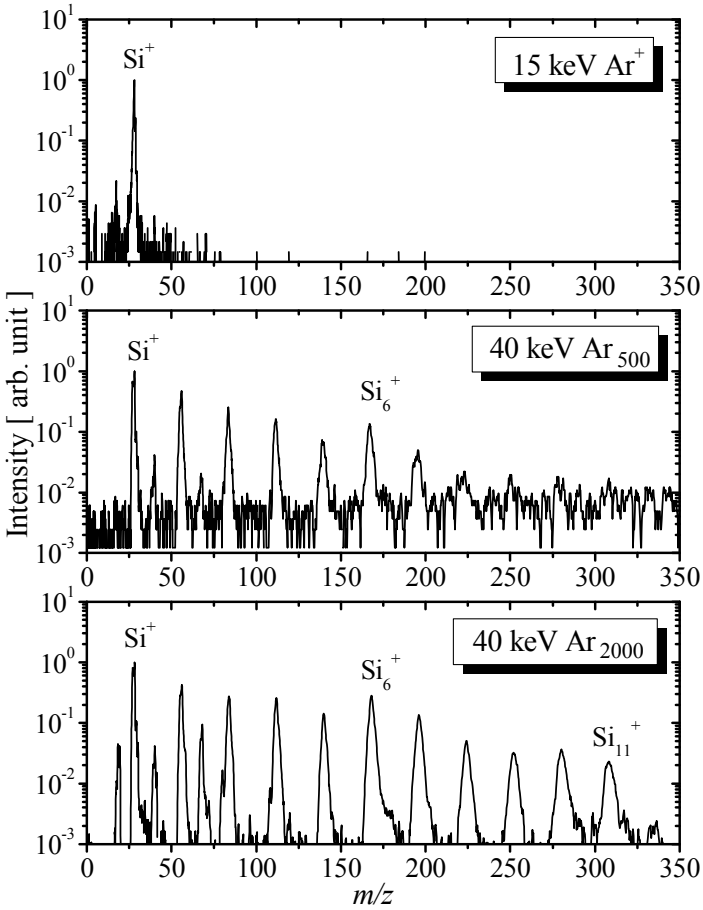

Fig. 2. Ninomiya et al. The emission process of secondary ions from solids bombarded with large gas cluster ions

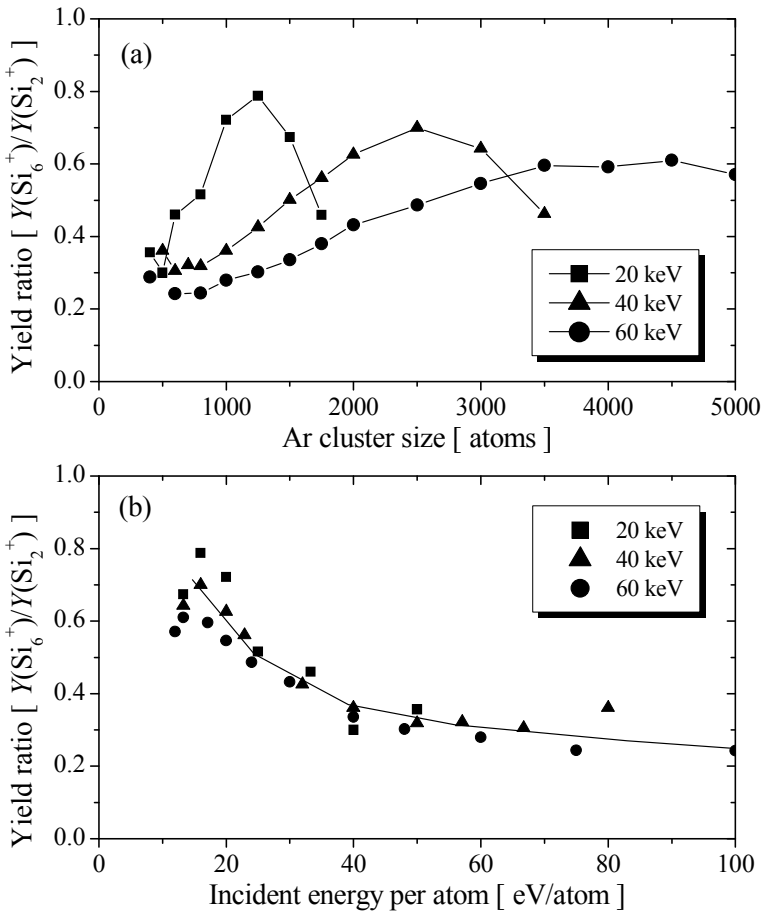

Fig. 3. Ninomiya et al. The emission process of secondary ions from solids bombarded with large gas cluster ions

.